Available online at www.sciencedirect.com
SCIENCE DIRECT
PALAEO
Palaeogeography, Palaeoclimatology, Palaeoecology 233 (2006) 149–162
www.elsevier.com/locate/palaeo

Millennial-scale Holocene climate variability in the NW China drylands and links to the tropical Pacific and the North Atlantic

Yongtao Yu [a,*], Taibao Yang [a], Jijun Li [a,b], Jinfeng Liu [a,c], Congrong An [a], Xiaoyan Liu [a], Zhe Fan [a], Zhenyu Lu [a], Yuanping Li [a], Xing Su [a]

[a] *National Laboratory of Western China's Environmental Systems, MOE, Lanzhou University, Lanzhou 730000, China*
[b] *College of Geography Science, Nanjing Normal University, Nanjing 210097, China*
[c] *Institute of Geology, China Earthquake Administration, State Key Laboratory of Earthquake Dynamics, Beijing 100029, China*

Received 15 December 2004; received in revised form 19 September 2005; accepted 21 September 2005

Abstract

A loess–paleosol sequence and a lake sediment record from the central Hexi Corridor in the drylands of NW China show patterns of persistent millennial- to centennial-scale climate variability during the Holocene epoch, which can be well correlated with abrupt climatic events reported from the North Atlantic and the Asian monsoon-dominated regimes. Our results show that the drylands in NW China might have been regulated both by the westerlies and by the East Asian summer monsoon (EASM) in a roughly synchronous manner. It seems that cold–dry intervals in the central Hexi Corridor may generally correspond to cooling phases in high latitudes of the Northern Hemisphere, and that cold/warm–wet intervals largely correlate with relatively warm phases in northern high latitudes. A candidate mechanism involving NAO/AO and ENSO dynamics is tentatively proposed to account for this synchroneity. Climatic patterns may be spatially different in the NW China drylands in response to the changing predominant control of either the westerlies or the EASM, depending on the contrast of their relative strengths. Glacier meltwater discharges associated with alpine warming may be partly responsible, at least for the two records discussed in this paper, for such spatial heterogeneity of climatic changes during the Holocene. More work is needed to evaluate the individual roles and combined impacts of the EASM, the westerlies and alpine glacier meltwater regulation on the NW China dryland dynamics.

Keywords: Millennial-scale climate variability; Holocene; NW China drylands; East Asian summer monsoon; Westerlies

1. Introduction

Unraveling the complex Holocene environmental responses to globally interlinked changes and understanding the respective roles of the different elements of the Earth's environmental systems represent major challenges to earth scientists (Sarnthein et al., 2002). To this end, stratigraphic evidence with resolution capable of recording high-frequency changes from climatically sensitive regions is essential for shaping general patterns of climatic change histories during key periods of the Holocene, and may contribute to the detailed understanding of causes and mechanisms of millennial- or finer scale variability in the mid-latitude Asian drylands. The vast drylands in NW China, and of central Asia as a whole, are located at the boundary between the East Asian summer monsoon (EASM) and the

* Corresponding author. Tel.: +86 931 891 3138; fax: +86 931 891 2642.
E-mail addresses: eaglespade@hotmail.com (Y. Yu), yangtb@lzu.edu.cn (T. Yang).

0031-0182/$ - see front matter © 2005 Elsevier B.V. All rights reserved.
doi:10.1016/j.palaeo.2005.09.008

Northern Hemisphere westerly winds (Lehmkuhl and Haselein, 2000; Yang and Williams, 2003). They are climatically sensitive regions which are likely to have experienced conditions during the Holocene which were quite different to those of the present (Fontes et al., 1996; Lehmkuhl and Haselein, 2000).

Previous work on NW China's drylands focused primarily on the Shiyang River drainage basin in the eastern Hexi Corridor (Chen et al., 1999, 2001; Zhang et al., 2000; Shi et al., 2002; Ma et al., 2003), the Badain Jaran Desert (Yang, 2000; Yang and Williams, 2003; Yang et al., 2004b), southern Inner Mongolia (Chen et al., 2003), and northern Xinjiang (Sun et al., 1994; Wünnemann et al., 2003). However, there is still a lack of evidence from the middle part of the Hexi Corridor, a key region that climatically links the EASM, the westerlies and the regulation of the Tibetan Plateau. An investigation of this region, integrated with previous reports from adjacent sites, will help us to understand general patterns, spatial heterogeneity and forcing mechanisms of Holocene climate changes over the east-central Asian drylands.

To this end we present a multiproxy reconstruction of the Holocene section of a 40-m-long sediment core (GT40 core) recovered from the Yanchi playa (39°45′ N, 99°18′ E), in the central Hexi Corridor in arid NW China. In addition, a 3-m-long loess section (BDK section) from Biandukou (38°13′ N, 100°52′ E), in the subalpine part of the eastern Qilian Shan, ~200 km southeast of the Yanchi playa, is chosen for a regional comparison. Because the Yanchi playa may be linked hydrologically via the Ruoshui River to the alpine glaciers in the eastern Qilian Shan, the BDK section serves as an important complementary archive to the GT40 record. First, alpine glaciers may respond sensitively to climatic changes of regional and/or global significance. Second, changes in glacier meltwater discharges in response to alpine warming may effectively regulate patterns of environmental changes in the downstream arid areas, namely the central Hexi Corridor. Third, by correlating these two records with regional and global climatic evidence we hope to contribute to the understanding of major factors that control the evolution of the central Asian drylands during the Holocene in the context of global changes.

Unless otherwise stated all ages, including those from cited references, are given in calendar yr/kyr before 1950 A.D. (cal. yr/kyr BP) with 2σ errors. Although the GT40 chronology is poorly constrained, our results suggest that millennial-scale abrupt climate variability may persist over east-central Asia during the entire Holocene. Through careful correlations we tentatively attribute this pattern to roughly synchronous operations of the westerlies and the EASM. Further work with finer sample resolution and refined chronology is needed to assess quantitatively and more precisely the specific signatures of these controlling factors and their combined impacts on the evolution of arid environments in NW China and the east-central Asia.

2. Study areas and methods

2.1. Physical settings and stratigraphy

The Yanchi playa, a tectonically subsiding basin, is located in the middle part of the Hexi Corridor (Fig. 1),

Fig. 1. Location map showing the positions of the study areas (B) relative to the northwestern China (A). 1: GT40 core from the Yanchi playa; 2: Biandukou (BDK) section in the eastern Qilian Shan. Light shaded areas represent the Badain Jaran Desert and the Tengger Desert.

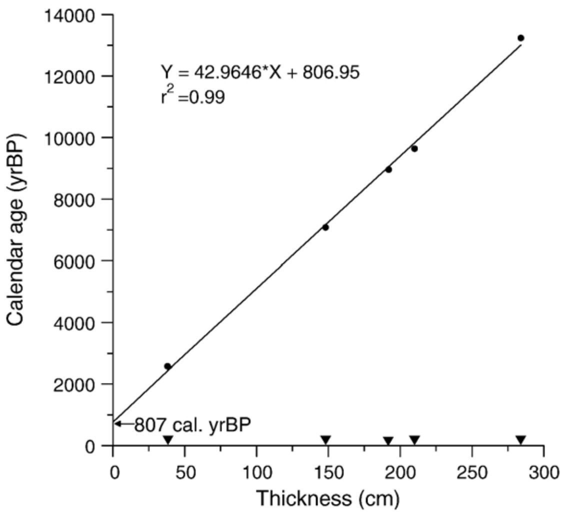

Fig. 2. The BDK age–depth relationship. The solid dots are calibrated calendar ages. The solid line indicates the linear regression age model based on 5 calibrated dates. Solid triangles indicate positions where dating samples are collected.

confined by the Heli-Longshou Shan to the northeast and the Qilian Shan to the southwest. Situated in the interior of Asian continent, it has a typical continental climate with modern mean annual temperature ca. 8 °C, mean annual precipitation ca. 110 mm and mean annual evaporation up to ca. 2400 mm. The Badain Jaran Desert and the Tengger Desert bound the Corridor on the northeast and the east, respectively. The Yanchi paleolake is estimated to have been formed no later than 140 kyr BP according to paleomagnetic dating, when the latest tectonic movement causes faulting within the massive alluvial fans on which this lake developed (Yang et al., 2004a).

Two sediment cores were drilled in 1999 in the Yanchi playa. The GT40 core was recovered from a near-shore location and the 60-m-long (GT60) core was drilled near the center of the playa some 500 m away from the GT40 site. The lithologies of the Holocene sections of these two cores show considerable differences. The GT60 core is interrupted by two sections of halite (NaCl crystals) deposition at depths between 0 and 237 cm and between 290 and 449 cm. Mirabilite ($NaSO_4 \cdot 10H_2O$) crystal layers are observed in the GT40 core between 474 and 682 cm; they are interbedded with undecomposed organic material and dark-grey peat. The second interval of mirabilite deposition occurs between 935 and 1110 cm, accompanied by clay/clayey silt rich in calcic carbonate nodules in the GT40 core. These differences may result from spatial differentiation of salt depositional process in the saline Yanchi paleolake. In this paper we focus on the Holocene section of the GT40 core in view of its sedimentary continuity.

The Biandukou (BDK) section (38°13′ N, 100°52′ E, 2840 m a.s.l.) is located on the third terrace some 27 m above the Tongziba River, which flows out of the Qilian Shan into the eastern Hexi Corridor (Fig. 1). Modern mean annual temperature at this site is about 3 °C and mean annual precipitation is about 400 mm. The BDK section is capped by a topmost 10-cm-thick modern soil. The terrace is overlain by a 380-cm-thick loess–paleosol sequence, in which 5 paleosols are visually identifiable. Within the Holocene section, there are 4 paleosols evident between 10 and 40 cm, 76 and 84 cm, 120 and 152 cm, and 190 and 212 cm, in addition to a weakly developed paleosol at 84–120 cm (Fig. 3).

2.2. Chronology

The age model for the BDK section is based on 5 conventional radiocarbon dates (see Fig. 2 and Table 1). We choose a linear regression model to convert depth to age in view of the relatively uniform mass accumulation rate. The very high r^2 (=0.99) suggests a nearly

Table 1
Radiocarbon dates and calendar age calibrations

Lab no.	Sample no.	Description of materials and sampling positions in depth	Conventional ^{14}C ages (radiocarbon yr BP)	2σ calendar ages maximum (midpoint) minimum (cal. yr BP)
8605	BDK-1	Bulk organic matter, 38 cm	2481 ± 60	2730 (2580) 2430
8606	BDK-2	Bulk organic matter, 148 cm	6209 ± 85	7270 (7075) 6880
8607	BDK-3	Bulk organic matter, 210 cm	8626 ± 80	9800 (9640) 9480
8608	BDK-4	Bulk organic matter, 248 cm	11,274 ± 100	13,470 (13,235) 13,000
031	BDK-5	Bulk organic matter, 192 cm	8070 ± 115	9290 (8960) 8630
8612	GTC-1	Bulk organic matter, 1624 cm	16,400 ± 540	20,952 (19,551) 18,197
		Reservoir corrected age	15,900 ± 540	20,372 (18,976) 17,634

Note: All samples were pretreated and measured at the laboratory of radiocarbon geochronology of Lanzhou University. Conversions of radiocarbon ages to calendar ages are worked out by using the CALIB4.3 program (Stuiver et al., 1998). The GTC-1 sample is taken from the GT40 core and the remaining 5 samples are from the BDK section.

constant dust accumulation rate in the eastern Qilian Shan during the Holocene. This may imply that these paleosols are accretionary in genesis, and that soil formation may operate contemporaneously with continuous accumulation of aeolian dusts. In response to the uniform dust accumulation, a soil profile may rapidly incorporate the newly deposited dusts to build up its horizon in a bottom-up fashion. A similar case is reported by Maher et al. (2003) from the western edge of the Chinese Loess Plateau.

It is worth noting that the extrapolated topmost age of the BDK section is ca. 807 yr BP, implying that the latest section might have been truncated for some reason, possibly through slope failure or strong surface erosion. Because it seems to be unlikely that the dust accumulation rate changed abruptly after 807 yr BP while remaining nearly constant before that time. In addition, the nearly complete removal of $CaCO_3$ from the uppermost 15 cm of sediment (Fig. 3) may indicate strong carbonate eluviation resulting from high precipitation which might in turn have removed the surface sediment.

The GT40 chronology is constructed by linear interpolation between a conventional radiocarbon date (16,400 ± 540 yr BP) on bulk sample organic matter, and the topmost sediment which is assumed to be "0 yr". Carbon reservoir correction was done by assuming a reservoir age of 500 yr that was reported by Chen et al. (2001) from the SJC section. Considering the very similar saline-lake nature of these two sites and the geographic vicinity, this method may be viable and can be improved by further dating efforts. The reservoir age was subtracted from the raw radiocarbon age and then converted to calendar years (Table 1). Although the chronological framework of the Holocene part of the GT40 core is poorly constrained, regional and global comparisons (see Results and discussion section) may partly support its validity.

2.3. Measurements and interpretations of climate proxies

All sediments were subjected to multiproxy analyses of magnetic, optical and geochemical properties at a 2-cm sampling interval. Low-frequency magnetic susceptibility (MS) was determined at 0.47 kHz using a Bartington MS2B susceptibility meter. Analyses of $CaCO_3$ were done using a Bascomb calcimeter. Grain size (GS) analyses were determined using a MasterSizer 2000 unit at the National Laboratory of Western China's Environmental Systems. Sediment color reflectance (SCR) parameters were measured on air-dried samples using an X-Rite 948 spectrophotometer with

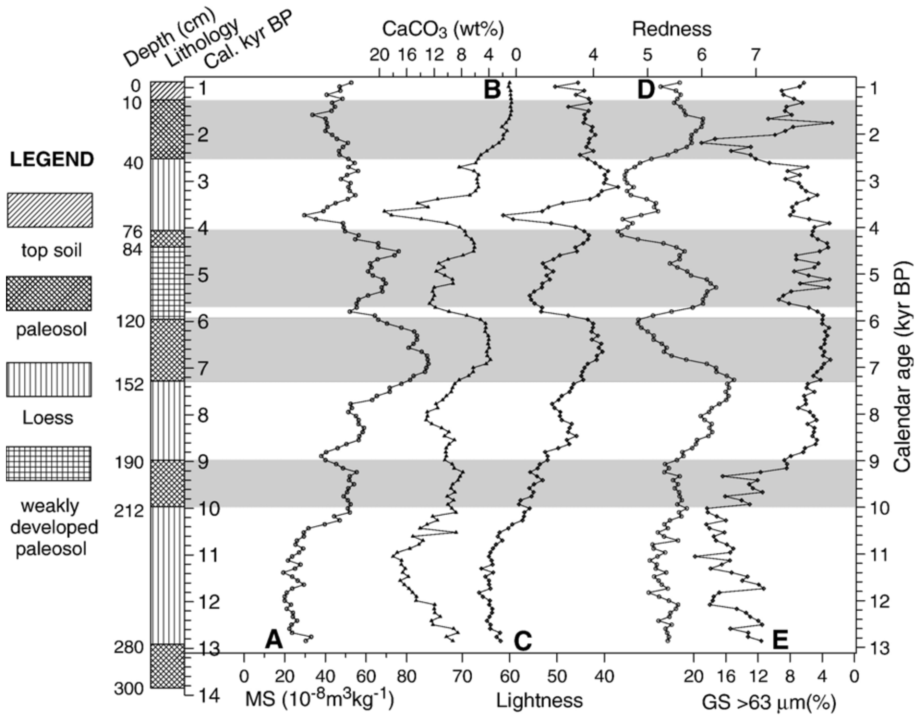

Fig. 3. Stratigraphy and climatic proxies of the Biandukou (BDK) section. Note that scales of curves B, C, E are reversed. Shaded areas indicate climatic events discussed in the text.

the D_{65} illuminant and a 10° observational horizon. The data are represented under the L*a*b* chromatic space by CIE 1976.

Sediment conductivity is a new proxy in this research. 1.0 g of air-dried, pestle-ground sample was dissolved in 50 ml distilled water, and sufficiently agitated to ensure total dissolution of soluble components. Prior to measurement, sample solutions were stored overnight at room temperature and then were measured using a Thermo Orion Model 555A conductivity meter. Although construction of quantitative relationships between conductivity of the sediment and that of the lake water is not pursued in this research, we tentatively argue that conductivity of these sediments should indirectly reflect the overall soluble salt concentration of the lake water that may be mainly controlled by moisture availability (ratio of precipitation to evaporation). In this paper, higher/lower conductivity is interpreted as a reflection of enhanced/decreased moisture availability.

Next we discuss the interpretation of the proxies used in this study. Coarse fraction GS of Chinese loess has been mainly used to reconstruct winter monsoon intensity. Because the BDK section lies very near the Badain Jaran Desert and the Tengger Desert, higher/lower GS (>63 μm fraction) percentage may actually reflect expansion/shrinkage of these deserts in response to enhanced/weakened winter monsoon. $CaCO_3$ content is also frequently used as an indicator of paleoenvironmental changes. However, interpretation of this proxy is not straightforward. For loess–paleosol sequences, the measured $CaCO_3$ content may be significantly affected by the processes of eluviation and illuviation. Because it seems very unlikely that the carbonate content of aeolian dusts varies markedly at this site over millennial-scales, we tentatively argue that lower measured $CaCO_3$ content may reflect stronger eluviation in response to enhanced precipitation. Higher $CaCO_3$ content may reflect either weaker eluviation caused by less rainfall, or later illuviation of carbonates from overlying deposits. In the latter case, the environmental significance of the measured $CaCO_3$ peak is unclear. Interpretation of $CaCO_3$ content of lake sediments, as in loess–paleosol sequences, is not straightforward. However, higher/lower $CaCO_3$ is generally assumed to reflect decreased/enhanced basin-scale moisture availability (Chen et al., 2001).

SCR parameters (redness and lightness) have been used by many researchers as environmental proxies. Lightness in general correlates positively with carbonate and opal content and negatively with organic matter content, and redness is primarily affected by hematite content controlled mainly by temperature (Fang et al., 1999; Giosan et al., 2002). Because it is hard to interpret the redness data of lake sediments due to the complexity of dynamic lake depositional environments, we only present those for the BDK loess–paleosol section to facilitate clearer interpretations. In this study, higher/lower redness represents higher/lower temperature in the alpine part of the eastern Qilian Shan. Higher/lower lightness represents lower/higher organic matter content, a reflection of drier/wetter conditions.

Low-frequency magnetic susceptibility (MS) is a useful climate proxy which has been widely used in paleoenvironmental reconstructions. In China, higher/lower MS is generally accepted as an indicator of ameliorated/deteriorated combinations of temperature and moisture availability in response to strengthened/weakened East Asian summer monsoon (EASM). We generally adopt this interpretation for the BDK loess–paleosol sequence. For the GT40 lake sediment record, this explanation is valid but other factors such as redeposition of detrital magnetic minerals that were eroded throughout the drainage basin (Evans and Heller, 2003) are likely to influence the signal.

3. Results and discussion

3.1. General patterns of climate changes

The climatic conditions of the central Hexi Corridor inferred from the GT40 proxies can be largely divided into four stages (Fig. 4): the fluctuating wet/dry Late Glacial; the generally humid early Holocene; the warm and humid Holocene Climate Optimum (HCO); the mid- to late-Holocene cooling and aridification alternating with spells of wetter conditions. Several common features are shared by these proxies. First, all proxies, except for conductivity, display significant fluctuations during the Late Glacial and the Holocene epoch, indicating that the central Hexi Corridor has experienced dramatic climate and environmental changes. Second, the general trends in MS, lightness and $CaCO_3$ are in agreement with the variation of the 60°N June insolation, indicating that changes in solar insolation might have exerted a strong influence on the environmental systems over this region. Third, as shown in Fig. 4, climates in the central Hexi Corridor gradually became much drier during the mid- and late-Holocene as evidenced by increased $CaCO_3$, lightness, conductivity and decreased MS. This aridification is so strong that after ca. 4700 yr BP average conductivity becomes almost 3 times greater than before. Halite

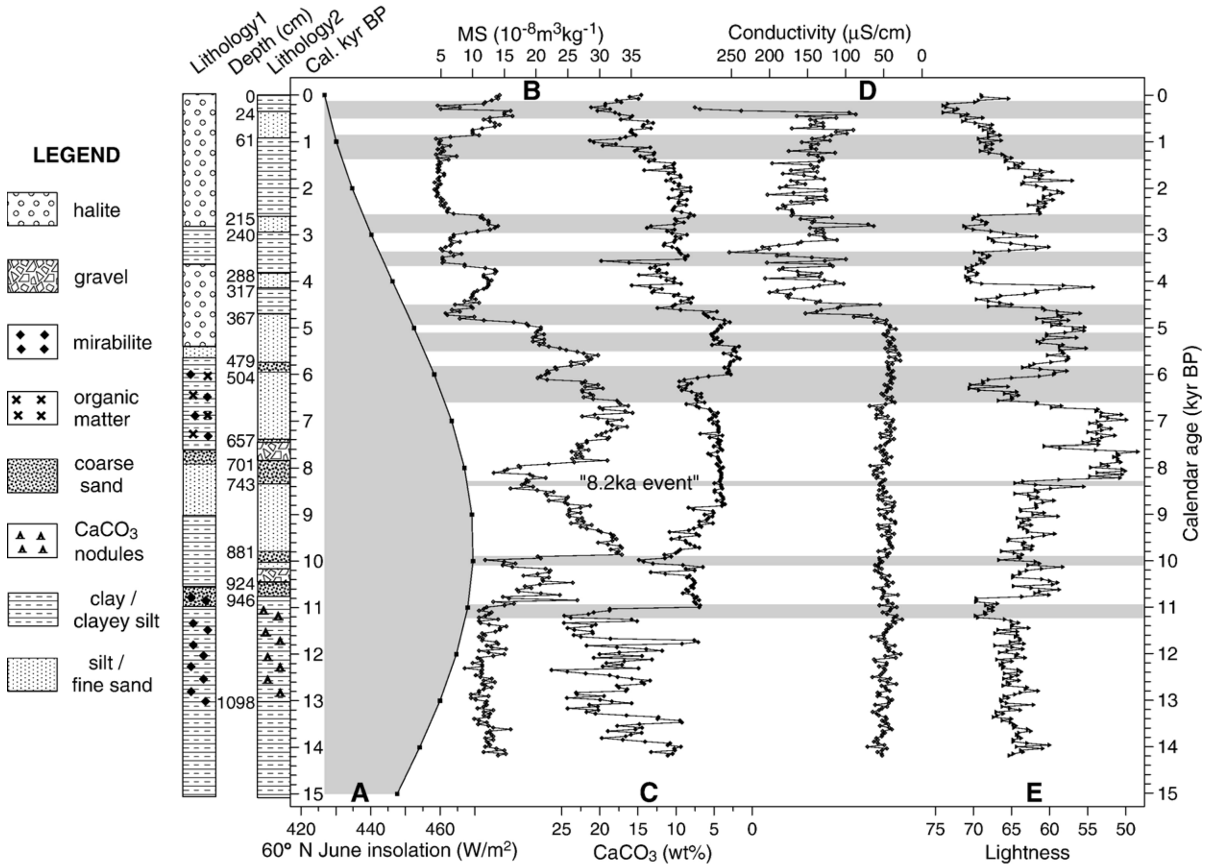

Fig. 4. Stratigraphy and climatic proxies of the Holocene section of the GT40 record. Lithology 1 is for the GT60 core and Lithology 2 is for the GT40 core. Shaded rectangular areas indicate abrupt cooling events discussed in the text. Note that scales of curves C, D, E are reversed. Curve A is drawn from Berger and Loutre (1991).

deposition is also evident in the GT60 core after that time. This may indicate the onset of a drastic desiccation process that finally drains the Yanchi paleolake. Finally, the above-mentioned general trends are superimposed by a series of climatic events marked by drier conditions that punctuate the entire Holocene, indicating the existence of millennial- to centennial-scale climatic fluctuations in the drylands of the central Hexi Corridor.

Despite the above-mentioned general agreements, the GT40 proxies show several dissimilarities that are worth noting. First, intervals with high MS generally correspond to silt/fine sand lithological units, while clay/clayey silt units are generally linked with low intervals of MS. This is also seen in the SJC section, where finer sediments have lower magnetic susceptibility signals (Chen et al., 2001). High MS corresponding to silt/fine sand units may result from terrigenous input of material rich in magnetic minerals. Second, MS and lightness are strikingly dissimilar during the early Holocene (ca. 9800–8300 yr BP) and during the late Holocene (especially at ca. 3400–1600 yr BP). During the former interval, the declining MS signal suggests a relatively warm and/or humid but gradually deteriorating environment that culminates at ca. 8200 yr BP, while the lightness proxy does not display large-amplitude fluctuations comparable to the MS record. This discrepancy may result from the difference of the properties of various proxies in responding to changing environment. Compared with the lightness record, which is interpreted as indicative of better moisture condition, the magnetic susceptibility record seems to be more temperature-dependent than moisture-sensitive. This is because both conductivity and $CaCO_3$, which are interpreted as reflections of better moisture conditions, are low and show little variation within this interval. During the latter interval, changes in these two proxies seem almost out of phase, i.e. higher/lower MS corresponds to lower/higher lightness. The actual causes of this phenomenon are still unknown and more investigation on the controls of these proxies is required.

Although high-frequency, short-lived events as evidenced by the GT40 proxies are relatively muted in the BDK loess section, possibly due to lower temporal resolution, millennial-scale climatic changes can also be identified in this profile (Fig. 3). The MS proxy generally correlates negatively with the lightness proxy, and with $CaCO_3$ content. At intervals when paleosols developed, climates in the Corridor side of the eastern Qilian Shan became ameliorated with enhanced moisture availability as evidenced by increased MS, decreased $CaCO_3$ and decreased lightness. The GS (>63 μm fraction) varies little during ca. 7000–6000 yr BP, suggesting a period of persistent desert retreat. A notable feature can be observed in Fig. 3. Before ca. 8000 yr BP redness is roughly in phase with MS, $CaCO_3$ and lightness, but after that time it becomes approximately 180° out of phase with the latter three proxies. As we interpret redness as temperature-dependent and lightness/$CaCO_3$ as moisture-sensitive, this change may indicate a climatic reorganization in terms of the configurations of temperature and precipitation: before this shift high/low temperature may be coupled with high/low moisture availability; while afterwards we assume the reverse case. An exception to this pattern occurs when the uppermost paleosol was formed (at ca. 2500–1200 yr BP). During this ca. 1300-yr-long unusual interval the GS (>60 μm fraction) first increases dramatically and then decreases drastically, indicating a rapid expansion of deserts followed by a rapid retreat. $CaCO_3$ is almost entirely leached and the peak of the redness proxy suggests a climate with increased temperature. This evidence may suggest that during ca. 2500–1200 yr BP the mountainous regions in the eastern Qilian Shan might have been climatically different from the nearby deserts.

Because the BDK section is hydrologically linked with the GT40 record, the moisture availability inferred from the GT40 lightness proxy may be linked with changes in temperature (inferred from the BDK redness proxy) in the alpine part of the eastern Qilian Shan through possible glacier meltwater regulations. Correlation of these two proxies (Fig. 5) confirms such a linkage because the three intervals of higher BDK redness (at ca. 8500–6700, ca. 5800–4300, and at ca. 2600–1600 yr BP) are roughly coeval with the three intervals of lower GT40 lightness (at ca. 8200–6700, ca. 6000–4500, and at ca. 2600–1600 yr BP) except for several intervals. It seems that glacier meltwater discharges in response to alpine warming do have an impact on the evolution of drylands in the Corridor.

3.2. Late Glacial–Holocene transition and the humid early Holocene

The Late Glacial climate over the central Hexi Corridor was characterized by rapid, large amplitude wet/dry fluctuations superimposed on a generally cold background, as witnessed in the significantly fluctuating $CaCO_3$ record. The presence of alternating mirabilite deposits in the GT60 core and the occurrence of $CaCO_3$ nodules in the GT40 core in sediments of the same age further support such highly unstable Late Glacial climates. This feature is also evident in the BDK section, in which the >63 μm GS fraction shows high-frequency, large amplitude oscillations during the Late Glacial and until ca. 9300 yr BP during the early Holocene. This may suggest that deserts in NW China (i.e., the Tengger Desert and/or the Badain Jaran Desert) might have undergone expansions and retreats during this period in response to frequent strengthening and weakening of the EASM. Our results are consistent with pollen and lacustrine stratigraphic evidence from the eastern Corridor (Shi et al., 2002; Ma et al., 2003).

The warm–humid phase between ca. 10,800 and 10,100 yr BP is mainly indicated by higher MS, much-reduced $CaCO_3$, and decreased lightness. The presence of coarse fluvial sands and angular gravel deposits in the GT40 core (see Fig. 4) during that period may reflect enhanced surface erosion caused by increased precipitation over the central Hexi Corridor. This humid phase is further supported by evidence from the adjacent Badain Jaran Desert (Yang, 2000) and north Xinjiang (Wu et al., 2003). However, pollen evidence from the eastern Hexi Corridor (Ma et al., 2003) indicates dry conditions at this time. This discrepancy may highlight either the spatial heterogeneity of Holocene environmental changes over the NW China drylands, or dating or correlation problems which need to be addressed by a refined chronology.

The above-mentioned warm–humid phase in the GT40 record was bracketed by two major cooling events. As shown in Fig. 5, the former cold–dry climatic event between ca. 11,200 and 10,900 yr BP roughly correlates with the IRD event 8. The latter cold–dry event between ca. 10,100 and 9900 yr BP is coherent with previous reports from NW China (Chen et al., 2001; Zhou et al., 2002), and with sites in northern Europe (Björck et al., 2001). It is also evident in the Guliya ice core $\delta^{18}O$ record (Thompson et al., 1997; Wang et al., 2002) and may be correlated with the IRD event 7 in the North Atlantic (Bond et al., 2001) within dating uncertainties. With respect to the YD event, the GT40 proxies do not provide evidence

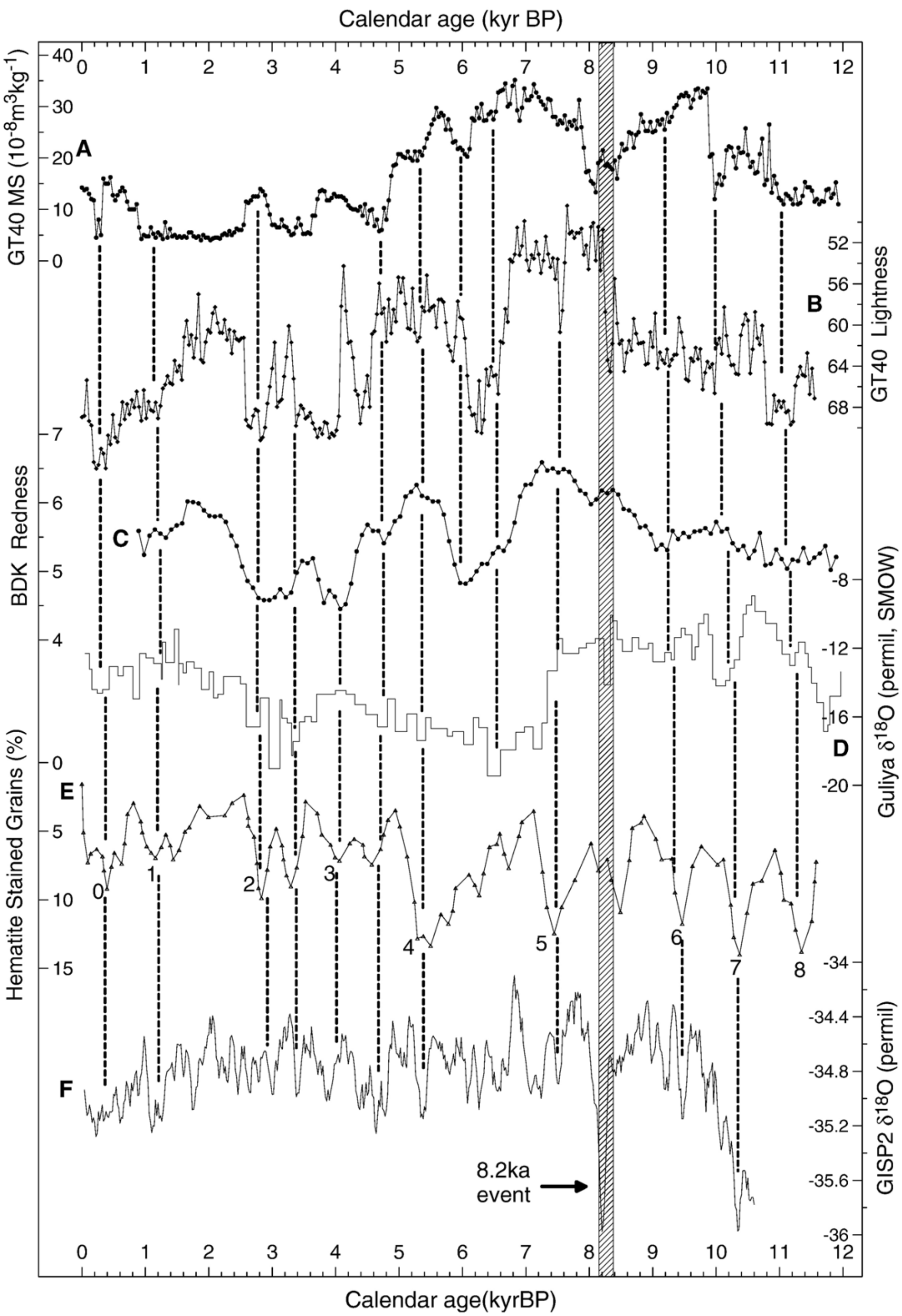

Fig. 5. Comparisons of the GT40 and the BDK records with global evidence. (A) GT40 magnetic susceptibility (MS); (B) GT40 lightness; (C) BDK redness; (D) Guliya ice core δ^{18}O record (Thompson et al., 1997); (E) stacked hematite stained grains from the North Atlantic IRD record (Bond et al., 2001), number of IRD events is assigned by the original authors; (F) 5-point running averaged Greenland GISP2 ice core δ^{18}O record (data provided by the National Geophysical Data Center). Note that scales of curve B and curve E are reversed.

indicating unfavorable climate conditions during that interval.

The warm–humid early Holocene over the central Hexi Corridor, in phase with western China and Mongolia (Yang et al., 2004b), commenced at ca. 10,000 yr BP and ended at ca. 8000 yr BP. During this interval a paleosol developed in the BDK section possibly under the influence of warmer and more humid climates. This warm–humid phase, in agreement with North Atlantic warming (Bauch et al., 2001) and boreal forest expansion (MacDonald et al., 2000), might have been forced by elevated atmospheric CO_2 and methane concentration during the early Holocene (Wagner et al., 1999; Smith et al., 2004), and might have been related to the operation of a NAO-like pattern conducive to strengthened westerly winds across the Northern Hemispheric mid-latitudes (Hoerling et al., 2001). A dry interval accompanied by a slight fall in temperature occurred between ca. 9300 and 9000 yr BP in the GT40 record, roughly coeval with evidence from adjacent regions (Chen et al., 2001; Wang et al., 2002; Zhou et al., 2002). This event, along with other short-lived abrupt cooling and drying events registered in the central Hexi Corridor during the Late Glacial and the early Holocene, may be correlative to freshwater discharges from the Laurentide Ice Sheet (Magny and Bégeot, 2004), suggesting possible links between climates in NW China and the North Atlantic region.

3.3. Early–mid-Holocene transition (EMHT) and the 8200-yr event

The warm–humid early Holocene recorded in the GT40 sediments was ended by a substantial cooling phase at ca. 8400–7800 yr BP (at ca. 8200–7600 yr BP in the BDK section), denoting the early- to mid-Holocene transition (EMHT). This event in the GT40 record may encompass two minor perturbations. The former, of a cold–dry nature at ca. 8400–8100 yr BP, correlates well with the so-called 8200-yr abrupt cooling event reported from the Guliya ice core, and the Greenland GISP2 ice core oxygen isotope record (Fig. 5). Our results and other evidence show that during this period the central Asian drylands experienced considerable cooling and drying (Zhang et al., 2000; Chen et al., 2001; Wang et al., 2002; Wünnemann et al., 2003; Ma et al., 2003; Yang and Williams, 2003). This signal, which is proposed to be partly propagated by the westerlies, may result from an upstream cooling by 4–8 °C in the North Atlantic triggered by catastrophic drainage of Laurentide lakes in the Laurentide Ice Sheet (LIS) to the North Atlantic and by subsequent collapse of the North Atlantic Thermohaline Circulation (Barber et al., 1999). This event may have greater implications for the drylands in NW China, taking into account the rather significant shift in climate patterns inferred from proxy analyses (see Section 3.1). More evidence with higher temporal resolution and environmentally explicit proxies is needed to evaluate more precisely the impact of the 8200-yr event on the central Asian drylands.

The ensuing cooling event after the 8200-yr event in the GT40 record occurred at ca. 8100–7800 yr BP according to our chronology, and was characterized by abrupt changes in temperature and enhanced moisture availability. It is coherent with an abrupt atmospheric circulation change at the EMHT (Stager and Mayewski, 1997). This atmospheric reorganization may mark a prominent shift in climatic forcing mechanisms over arid NW China during the EMHT, when solar insolation outweighed glacial boundary conditions as the primary factor in directly forcing the Indian summer monsoon and the North American climates (Fleitmann et al., 2003). Although the 8200-yr event and the ensuing EMHT event are both evident in the GT40 record, the quality of the chronology and the relatively low resolution of the BDK record make such correlation more or less tentative. Whether these two perturbations represent true, separate climatic events or not entails further investigations over the study area.

3.4. The mid-Holocene

The Holocene Megathermal period in the GT40 record at ca. 7800–6200 yr BP is roughly correlative with the Holocene Climate Optimum (HCO) at ca. 8000–6600 yr BP, although both are punctuated by a series of significant climatic events at ca. 7600–7400, 6600–5800, 5500–5100, 4900–4500 and 4500–4200 yr BP (Fig. 5). Maximum temperature may have been attained around 7000 yr BP, and then decreased toward long-term cooling that culminated at ca. 4600 yr BP. The Megathermal period of the BDK record was between ca. 7800 and 6800 yr BP, while the HCO was between ca. 7600 and 6200 yr BP.

We assume that the onset and termination of the HCO in the central Hexi Corridor occur significantly earlier than in the eastern Qilian Shan, in agreement with the conclusions of previous research (He et al., 2004). Large-scale withdrawal of the EASM that causes termination of the HCO might have commenced shortly after ca. 8000–7000 yr BP in northern Xinjiang and the Tibetan Plateau (Wei and Gasse, 1999), at about 6600 yr BP in the central Hexi Corridor (GT40 record), ~6500 yr BP in the eastern Hexi Corridor (Zhang et al., 2000),

~6200 yr BP in the eastern Qilian Shan (BDK section), and at ca. 4000 yr BP in the western part of the Chinese Loess Plateau (Feng et al., 2004). This gradual seaward shift of the HCO termination is roughly in phase with the progressive weakening of the summer monsoon as the summer solar radiation anomaly decreases progressively through the Holocene (An et al., 2000).

A dry/wet couplet may be one of the most drastic changes in climate during the mid-Holocene. The former dry interval at ca. 6600–6100 yr BP was followed by a transient wet spell at ca. 6100–5800 yr BP. Evidence supporting the first dry interval is widely seen in the NW China drylands (Sun et al., 1994; Zhang et al., 2000; Chen et al., 2003; Ma et al., 2003) and in NW India (Enzel et al., 1999). The prevalence of this drying event suggests that the NW China may lie beyond the reach of major monsoonal precipitation, when the Asian summer monsoons may be greatly weakened. During the ensuing wet phase centered on ca. 6000 yr BP, climate over the central Hexi Corridor became much more humid. The eastern Qilian Shan was also characterized by relatively cool and humid climates (Fig. 3). In the meanwhile, prevalent high lake levels were evident across the Asian continent (Qin and Yu, 1998). The EASM might have been strengthened at that time and shifted northward for about 300–500 km than at 9000 yr BP (Harrison et al., 1996). The summer monsoon rainfall in North Africa was also greatly enhanced by more than 25% concurrently (Kutzbach and Liu, 1997). This prevalent 6000-yr event, characterized by enhanced moisture availability due to strengthened Asian summer monsoons, might have been forced by the enhanced seasonal cycle of solar insolation in the Northern Hemisphere (Kutzbach and Liu, 1997). However, identification of the 6000-yr event recorded in the GT40 record seems to be somewhat tentative taking into account the quality of the chronology.

The dry interval at ca. 5500–5100 yr BP in the GT40 record is broadly supported by evidence from the Asian continent (Enzel et al., 1999; Fontugne et al., 1999; Shi et al., 2002; Wünnemann et al., 2003).This event roughly correlates with a synchronous cooling in the North Atlantic and Greenland (Fig. 5). Weakening of the Indian summer monsoon (Hong et al., 2003) and the South China Sea SSS minima (Wang et al., 1999) may also indicate that the Asian summer monsoons are weakened owing to reduced surface evaporation and subsequent reduction in water vapor transport northwestward to inland Asia, leading to a much drier condition in NW China.

The most prominent, two-step climatic degradation during the mid-Holocene in the GT40 record occurred between ca. 4900 and 4500 yr BP and the ensuing phase between 4500 and 4200 yr BP. The fact that all proxies show dramatic, rapid changes (Fig. 4) in the first step clearly points to an unprecedented environmental deterioration in the late mid-Holocene. This deterioration seems to be mainly characterized by severe cooling and moderate drying as evidenced by a sharp drop in MS, which may be more temperature-dependent than moisture-sensitive (see Section 3.1). This severe cooling was then followed by a drastic aridification. Evidence from the east-central Asian drylands (Sun et al., 1994; Zhang et al., 2000; Chen et al., 2001; Shi et al., 2002; Xiao et al., 2002; Yang and Williams, 2003) and from the Arabian Peninsula (Bray and Stokes, 2003), agrees well with our results. The collapse of ancient civilizations in north China (Jin and Liu, 2002; Wu and Liu, 2004) in response to such environmental deterioration further indicates that the EASM, along with the Indian summer monsoon, might have been greatly weakened at approximately the same time.

Such a significant monsoon weakening might have been caused by the establishment of the modern ENSO band (Moy et al., 2002) characterized by increased El Niño frequency and by changes in the location of convection in the Pacific Ocean (Morrill et al., 2003). The southward migration of the Intertropical Convergence Zone (ITCZ) after ca. 5400 yr BP (Haug et al., 2001), along with the above-mentioned ENSO operation may in turn be regulated by orbitally induced insolation in the tropical oceans (Hoerling et al., 2001; Fleitmann et al., 2003). In view of the universality of this event across the globe, we propose that the dramatic mid-Holocene deterioration was forced by the same triggering mechanism, possibly variations in solar insolation.

3.5. Late Holocene cooling and aridification

The late Holocene in the central Hexi Corridor was generally characterized by the predominance of colder and/or drier conditions alternating with several wetter/warmer spells. This trend of aridification is evident in both the GT40 and the BDK records (see Figs. 3 and 4), and in the Asian continent (Starkel, 1998). It may be associated with decreasing Northern Hemispheric solar insolation (Berger and Loutre, 1991). Maximum aridity in the GT40 record lasted for about 1000 years from ca. 4500 to 3500 yr BP, and was interrupted by a transient wet spell at ca. 4200 yr BP. This maximum drought interval is consistent with evidence for widespread maximum aridity at ca. 4500–3500 yr BP from lakes in northern Xinjiang and the Tibetan Plateau (Gasse et al., 1996; Rhodes et al., 1996; Wei and Gasse, 1999), and by evidence from adjacent regions (Chen et al., 1999; Zhang et al., 2000; Shi et al., 2002; Ma et al., 2003; Yang and Williams, 2003), indicating that this drought phase may be ubiquitously evident over the NW China and may have been linked to a markedly weakened EASM.

After this prolonged dry interval, a prominent wet event occurred between ca. 3400 and 3000 yr BP, interrupted by a short drying spell centered at ca. 3100 yr BP. This generally wet phase is also coherent with pollen evidence from the Tengger Desert (Zhang et al., 2000; Ma et al., 2003). The transient dry pulse is roughly coeval with the most severe cooling event recorded in the Guliya ice core during the late Holocene (Thompson et al., 1997; Wang et al., 2002), and is coherent with an abrupt sedimentary transition from a mid-Holocene sapropel to calcareous laminated muds which occurred at about 3200 yr BP in Lake Bosumtwi, Ghana, western Africa (Russell et al., 2003). It may have been forced by internal atmospheric variability as shown by a model simulation (Hall and Stouffer, 2001). Taking into account the quality of the chronology and the briefness of this drying spell, we are not certain if it is a real reflection of a climatic event of global significance or just a local signature although the above correlation seems plausible. When the IRD event 3 occurred, the Guliya ice core recorded a high temperature but the BDK record showed cooling which was consistent with the drying interval in the GT40 record. This may be caused by differences in the properties of these proxies or by imprecision of the chronology.

The most humid period during the late Holocene over the central Hexi Corridor occurred at ca. 2600–1600 yr BP. It coincides with a warmer climate over the eastern Qilian Shan, and is supported by sand-dune destabilization (Yang, 2000) and by widespread alluvial fan formation in the central part of Turkey (Kashima, 2002). During this period, climates over the North Atlantic also became relatively warmer. Prior to this major humid phase there occurred a dry interval at ca. 3000–2600 yr BP, which was in phase with dune reactivation in the Arabian Peninsula (Bray and Stokes, 2003), and with cooling in the Guliya ice core and the North Atlantic IRD event 2 (Fig. 5).

The most recent two drying events occurred at ca. 1400–900 and ca. 500–150 yr BP (Fig. 5). The first dry interval in the GT40 record is in phase with collapses of ancient civilizations in central and South America in response to persistent, long-term drought (deMenocal, 2001), possibly suggesting coherent climate controls in the circum-Pacific regions. The latter one, along with the preceding warming phase at ca. 900–450 yr BP, is tentatively correlated to the Little Ice Age (LIA) and the Medieval Warm Period (MWP), respectively. Although the relatively poor age control and inadequate sample resolution may preclude convincing correlations of these two events, they do largely agree with the MWP and LIA reported from central China (Paulsen et al., 2003) and the Tibetan Plateau (Yang et al., 2003). We tentatively propose that the following three factors may account for the cold–dry conditions during the LIA in the central Hexi Corridor: (1) decreased Northern Hemispheric temperature (Shindell et al., 2001); (2) strengthened Asian summer monsoon circulation due to an increased latitudinal temperature gradient (Anderson et al., 2002); and (3) reduced water vapor transport resulting from decreased SSTs in the tropical oceans (deMenocal et al., 2000; Hendy et al., 2002).

4. Synchronous operations of the westerlies and the EASM over the east-central Asian drylands

The results from the GT40 and BDK records and the suggested correlations (Fig. 5) may indicate the global nature of these recurring millennial-scale events and the possible links between arid NW China and the North Atlantic region. As shown in Fig. 5, most of the climatic events recorded in the GT40 core are mainly characterized by cooling/drying conditions which are comparable to concurrent cooling in the North Atlantic and Greenland. The wet/warm intervals are primarily correlated to relatively warm periods in the northern high latitudes. However, the IRD event 4 and 5 and the intermediate period are different from the above pattern and deserve special attention. When these two events occurred, cold climates dominated the northern high latitudes in contrast to generally warmer/wetter climates in the central Hexi Corridor (Fig. 5). The intermediate period is characterized by a generally warmer climate in the northern high latitudes but by a colder/dryer climate in the central Corridor. The actual causes of the discrepancy remain elusive but may associate with the climatic reorganization induced by the 8200-yr event. Despite this dissimilarity, we tentatively propose that the east-central Asian drylands, including NW China, may be climatically regulated by co-operation of these two circulation systems in a roughly synchronous way.

Our proposal of a synchronous control is supported by increasing evidence from these two key regions. The South China Sea (Kienast et al., 2001), the Indian monsoon-dominated region (Enzel et al., 1999; Goodbred and Kuehl, 2000), and the Nordic Seas in the North Atlantic (Bauch et al., 2001) all experienced warming during the period ca. 10,000–6000 yr BP. The

South China Sea witnessed cooling synchronous with the North Atlantic during the YD period (Steinke et al., 2001), and also exhibited behavior parallel to Greenland warming (Kienast et al., 2001). Speleothem evidence from eastern China also revealed a pattern of reduced summer monsoon moisture at times when Greenland was experiencing stadial conditions (Wang et al., 2001). Weakening of the Indian summer monsoon coincides with cold intervals recorded in the North Atlantic (Fleitmann et al., 2003; Gupta et al., 2003; Hong et al., 2003). Simulations also show teleconnections between the North Atlantic and the North Pacific when the North Atlantic Deep Water Formation was weakened (Mikolajewicz et al., 1997). The Northern Hemisphere underwent almost synchronous changes during the last glacial termination (Benson et al., 1997; Hoerling et al., 2001).

We tentatively propose the following mechanism to explain this synchroneity. When the northern high latitudes are cooled, a negative state of the NAO/AO leads to weakened, southward displaced westerlies (Magny et al., 2003; Magny and Bégeot, 2004) with reduced water vapor delivery to the Asian hinterland in combination with an intensified, southward-expanded polar vortex (Arz et al., 2001). El Niño-like patterns in the tropical Pacific, which are concurrent with southward migrated ITCZ (Haug et al., 2001; Lea et al., 2003), function in concert with greatly weakened Asian summer monsoon (Stott et al., 2002), drawing moisture away from the Asian-side of the Pacific. The east-central Asian drylands may have undergone severe cooling and persistent, long-term drought owing to concurrently reduced moisture availability from both the Atlantic and the Pacific. Conversely, when the Northern Hemisphere high-latitudes get warmed, a positive mode of the NAO/AO causes northward displaced, stronger-than-average mid-latitude westerlies (Hoerling et al., 2001) with an enhanced latitudinal water vapor gradient into the central Asian drylands. Synchronously, the La Niña-like mode of ENSO accompanied by northward displaced ITCZ causes strengthened Asian summer monsoons, bringing more precipitation to the Asian-side of the Pacific. The east-central Asia therefore experiences ameliorated environmental conditions with enhanced moisture availability and reduced drought length and frequency. Spatial heterogeneity of climatic changes in this region is attributed to relative strength contrast of these two circulation systems, and to potential regulation of glacier meltwater discharges owing to alpine warming. More work with refined chronology and environmental-explicit proxies is needed to test the above hypothetic mechanism.

5. Conclusions

Our reconstructions of paleoclimate and paleoenvironment over the central Hexi Corridor provide evidence for a highly variable Holocene in drylands in NW China. On the basis of the aforementioned discussions several conclusions can be drawn as follows: (1) our proxy analysis and correlations show that the arid regions in NW China have undergone persistent millennial-scale climatic fluctuations; (2) these drylands might have been modulated both by the East Asian summer and winter monsoons, and by the westerlies in a roughly synchronous way; and (3) glacial meltwater discharges associated with alpine warming may partly contribute to the dryland spatial heterogeneity of climatic changes during the Holocene.

Acknowledgements

This research is financially supported by the National Natural Science Foundation of China (NSFC, Grant No. 49731010). Nai' ang Wang, Congrong An, and Haibin Wang offered assistances during field coring. We sincerely thank Dr. Jan Bloemendal, Dr. Bernd Wünnemann and an anonymous reviewer for their valuable suggestions and comments which greatly improved the original manuscript. We also owe a debt of gratitude to Baorong Xu and Shumin Fang for their assistance in analyzing samples from the GT40 and the BDK section.

References

An, Z.S., Porter, S.C., Kutzbach, J.E., Wu, X.H., Wang, S.M., Liu, X.D., Li, X.Q., Zhou, W.J., 2000. Asynchronous Holocene optimum of the East Asian monsoon. Quat. Sci. Rev. 19, 743–762.

Anderson, D.M., Overpeck, J.T., Gupta, A.K., 2002. Increase in the Asian southwest monsoon during the past four centuries. Science 297, 596–599.

Arz, H.W., Gerhardt, S., Pätzold, J., Röhl, U., 2001. Millennial-scale changes of surface- and deep-water flow in the western tropical Atlantic linked to Northern Hemisphere high-latitude climate during the Holocene. Geology 29 (3), 239–242.

Barber, D.C., Dyke, A., Hillaire-Marcel, C., Jennings, A.E., Andrews, J.T., Kerwin, M.W., Bilodeau, G., McNeely, R., Southon, J., Morehead, M.D., Gagnon, J.-M., 1999. Forcing of the cold event of 8200 years ago by catastrophic drainage of Laurentide lakes. Nature 400, 344–348.

Bauch, H.A., Erlenkeuser, H., Spielhagen, R.F., Struck, U., Matthiessen, J., Thiede, J., Heinemeier, J., 2001. A multiproxy reconstruction of the evolution of deep and surface waters in the subarctic Nordic seas over the last 30,000 yr. Quat. Sci. Rev. 20, 659–678.

Benson, L., Burdett, J., Lund, S., Kashgarian, M., Mensing, S., 1997. Nearly synchronous climate change in the Northern Hemisphere during the last glacial termination. Nature 388, 263–265.

Berger, A., Loutre, M.F., 1991. Insolation values for the climate of the last 10 million of years. Quat. Sci. Rev. 10, 297–317.

Björck, S., Muscheler, R., Kromer, B., Andresen, C.S., Heinemeier, J., Johnsen, S.J., Conley, D., Koç, N., Spurk, M., Veski, S., 2001. High-resolution analyses of an early Holocene climate event may imply decreased solar forcing as an important climate trigger. Geology 29 (12), 1107–1110.

Bond, G., Kromer, B., Beer, J., Muscheler, R., Evans, M.N., Showers, W., Hoffmann, S., Lotti-Bond, R., Hajdas, I., Bonani, G., 2001. Persistent solar influence on North Atlantic climate during the Holocene. Science 294, 2130–2136.

Bray, H.E., Stokes, S., 2003. Chronologies for Late Quaternary barchan dune reactivation in the southeastern Arabian Peninsula. Quat. Sci. Rev. 22, 1027–1033.

Chen, F.H., Shi, Q., Wang, J.M., 1999. Environmental changes documented by sedimentation of Lake Yiema in arid China since the Late Glaciation. J. Paleolimnol. 22, 159–169.

Chen, F.H., Zhu, Y., Li, J.J., Shi, Q., Jin, L.Y., Wünemann, B., 2001. Abrupt Holocene changes of the Asian monsoon at millennial- and centennial-scales: evidence from lake sediment document in Minqin Basin, NW China. Chin. Sci. Bull. 46 (23), 1942–1947.

Chen, F.H., Wu, W., Holmes, J.A., Madsen, D.B., Zhu, Y., Jin, M., Oviatt, C.G., 2003. A mid-Holocene drought interval as evidenced by lake desiccation in the Alashan Plateau, Inner Mongolia, China. Chin. Sci. Bull. 48 (14), 1401–1410.

deMenocal, P.B., 2001. Cultural responses to climate change during the late Holocene. Science 292, 667–673.

deMenocal, P., Ortiz, J., Guilderson, T., Sarnthein, M., 2000. Coherent high- and low-latitude climate variability during the Holocene warm period. Science 288, 2198–2202.

Enzel, Y., Ely, L.L., Mishra, S., Ramesh, R., Amit, R., Lazar, B., Rajaguru, S.N., Baker, V.R., Sandler, A., 1999. High-resolution Holocene environmental changes in the Thar Desert, Northwestern India. Science 284, 125–128.

Evans, M.E., Heller, F., 2003. Environmental Magnetism: Principles and Applications of Enviromagnetics Science. Academic Press, Amsterdam.

Fang, X.M., Yugo, O., Hitoshi, F., Pan, B.T., Li, J.J., Guan, D.H., Keiichi, O., Sumiko, T., Masayuki, T., Toshiaki, M., 1999. Asian summer monsoon instability during the past 60000 years: magnetic susceptibility and pedogenic evidence from the eastern Chinese Loess Plateau. Earth Planet. Sci. Lett. 168, 219–232.

Feng, Z.-D., An, C.B., Tang, L.Y., Jull, A.J.T., 2004. Stratigraphic evidence of a Megahumid climate between 10,000 and 4000 years B.P. in the western part of the Chinese Loess Plateau. Glob. Planet. Change 43, 145–155.

Fleitmann, D., Burns, S.J., Mudelsee, M., Neff, U., Kramers, J., Mangini, A., Matter, A., 2003. Holocene forcing of the Indian monsoon recorded in a stalagmite from southern Oman. Science 300, 1737–1739.

Fontes, J.C., Gasse, F., Gilbert, E., 1996. Holocene environmental changes in Lake Bangong basin (Western Tibet): Part 1. Chronology and stable isotopes of carbonates of a Holocene lacustrine core. Palaeogeogr. Palaeoclimatol. Palaeoecol. 120, 25–47.

Fontugne, M., Kuzucuoğlu, C., Karabiyikoğlu, M., Hatté, C., Pastre, J.-F., 1999. From Pleniglacial to Holocene: a ^{14}C chronostratigraphy of environmental changes in the Konya Plain, Turkey. Quat. Sci. Rev. 18, 573–591.

Gasse, F., Fontes, J.C., Van Campo, E., Wei, K., 1996. Holocene environmental changes in Bangong Co basin (Western Tibet): Part 4. Discussion and conclusions. Palaeogeogr. Palaeoclimatol. Palaeoecol. 120, 79–92.

Giosan, L., Flood, R.D., Aller, R.C., 2002. Paleoceanographic significance of sediment color on western North Atlantic drifts: I. Origin of color. Mar. Geol. 189, 25–41.

Goodbred Jr., S.L., Kuehl, S.A., 2000. Enormous Ganges–Brahmaputra sediment discharge during strengthened early Holocene monsoon. Geology 28 (12), 1083–1086.

Gupta, A.K., Anderson, D.M., Overpeck, J.T., 2003. Abrupt changes in the Asian southwest monsoon during the Holocene and their links to the North Atlantic Ocean. Nature 421, 354–357.

Hall, A., Stouffer, R.J., 2001. An abrupt climate event in a coupled ocean–atmosphere simulation without external forcing. Nature 409, 171–174.

Harrison, S.P., Yu, G., Tarasov, P.E., 1996. Late Quaternary lake-level record from northern Eurasia. Quat. Res. 45, 138–159.

Haug, G.H., Hughen, K.A., Sigman, D.M., Peterson, L.C., Röhl, U., 2001. Southward migration of the Intertropical Convergence Zone through the Holocene. Science 293, 1304–1308.

He, Y., Theakstone, W.H., Zhang, Z.L., Zhang, D., Yao, T.D., Chen, T., Shen, Y.P., Pang, H.X., 2004. Asynchronous Holocene climatic change across China. Quat. Res. 61, 52–63.

Hendy, E.J., Gagan, M.K., Alibert, C.A., McCulloch, M.T., Lough, J.M., Isdale, P.J., 2002. Abrupt decrease in tropical Pacific sea surface salinity at end of Little Ice Age. Science 295, 1511–1514.

Hoerling, M.P., Hurrell, J.W., Xu, T.Y., 2001. Tropical origins for recent North Atlantic climate change. Science 292, 90–92.

Hong, Y.T., Hong, B., Lin, Q.H., Zhu, Y.X., Shibata, Y., Hirota, M., Uchida, M., Leng, X.T., Jiang, H.B., Xu, H., Wang, H., Yi, L., 2003. Correlation between Indian Ocean summer monsoon and North Atlantic climate during the Holocene. Earth Planet. Sci. Lett. 211, 371–380.

Jin, G.Y., Liu, D.S., 2002. Mid-Holocene climate change in north China, and the effect on cultural development. Chin. Sci. Bull. 47 (5), 408–413.

Kashima, K., 2002. Environmental and climatic changes during the last 20,000 years at Lake Tuz, central Turkey. Catena 48, 3–20.

Kienast, M., Steinke, S., Stattegger, K., Calvert, S.E., 2001. Synchronous tropical South China Sea SST change and Greenland warming during deglaciation. Science 291, 2132–2134.

Kutzbach, J.E., Liu, Z., 1997. Response of the African monsoon to orbital forcing and ocean feedbacks in the middle Holocene. Science 278, 440–443.

Lea, D.W., Pak, D.K., Peterson, L.C., Hughen, K.A., 2003. Synchroneity of tropical and high-latitude Atlantic temperatures over the Last Glacial Termination. Science 301, 1361–1364.

Lehmkuhl, F., Haselein, F., 2000. Quaternary paleoenvironmental change on the Tibetan Plateau and adjacent areas (Western China and Western Mongolia). Quat. Int. 65/66, 121–145.

Ma, Y.Z., Zhang, H.C., Pachur, H.-J., Wünnemann, B., Li, J.J., Feng, Z.D., 2003. Late Glacial and Holocene vegetation history and paleoclimate of the Tengger Desert, northwestern China. Chin. Sci. Bull. 48 (14), 1457–1463.

MacDonald, G.M., Velichko, A.A., Kremenestki, C.V., Borisova, O.K., Goleva, A.A., Andreev, A.A., Cwynar, L.C., Riding, R.T., Forman, S.L., Edwards, T.W.D., Aravena, R., Hammarlund, D., Szeicz, J.M., Gattaulin, V.N., 2000. Holocene treeline history and climate change across Northern Eurasia. Quat. Res. 53, 302–311.

Magny, M., Bégeot, C., 2004. Hydrological changes in the European midlatitudes associated with freshwater outbursts from Lake Agassiz during the Younger Dryas event and the early Holocene. Quat. Res. 61, 181–192.

Magny, M., Bégeot, C., Guiot, J., Peyron, O., 2003. Contrasting patterns of hydrological changes in Europe in response to Holocene climate cooling phases. Quat. Sci. Rev. 22, 1589–1596.

Maher, B.A., Hu, M.Y., Roberts, H.M., Wintle, A.G., 2003. Holocene loess accumulation and soil development at the western edge of the Chinese Loess Plateau: implications for magnetic proxies of paleorainfall. Quat. Sci. Rev. 22, 445–451.

Mikolajewicz, U., Crowley, T.J., Schiller, A., Voss, R., 1997. Modeling teleconnections between the North Atlantic and North Pacific during the Younger Dryas. Nature 387, 384–387.

Moy, C.M., Seltzer, G.O., Rodbell, D.T., Anderson, D.M., 2002. Variability of El Niño/Southern Oscillation activity at millennial timescales during the Holocene epoch. Nature 420, 162–165.

Morrill, C., Overpeck, J.T., Cole, J.E., 2003. A synthesis of abrupt changes in the Asian summer monsoon since the last deglaciation. Holocene 13 (4), 465–476.

Paulsen, D.E., Li, H.-C., Ku, T.-L., 2003. Climate variability in central China over the last 1270 years revealed by high-resolution stalagmite records. Quat. Sci. Rev. 22, 691–701.

Qin, B.Q., Yu, G., 1998. Implications of lake level variations at 6 ka and 18 ka in mainland Asia. Glob. Planet. Change 18, 59–72.

Rhodes, T.E., Gasse, F., Lin, R.F., Ruifen, L., Fontes, J.-C., Wei, K.Q., Bertrand, P., Gilbert, E., Mélières, F., Tucholka, P., Wang, Z.X., Cheng, Z.-Y., 1996. A Late Pleistocene–Holocene lacustrine record from Lake Manas, Zunggar (northern Xinjiang, western China). Palaeogeogr. Palaeoclimatol. Palaeoecol. 120, 105–121.

Russell, J., Talbot, M.R., Haskell, B.J., 2003. Mid-Holocene climate change in Lake Bosumtwi, Ghana. Quat. Res. 60, 133–141.

Sarnthein, M., Kennett, J.P., Allen, J.R.M., Beer, J., Grootes, P., Laj, C., McManus, J., Ramesh, R., SCOR-IMAGES Working Group 117, 2002. Decadal-to-millennial-scale climate variability — chronology and mechanisms: summary and recommendations. Quat. Sci. Rev. 21, 1121–1128.

Shi, Q., Chen, F.H., Zhu, Y., Madsen, D., 2002. Lake evolution of the terminal area of Shiyang River drainage in arid China since the last glaciation. Quat. Int. 93/94, 31–43.

Shindell, D.T., Schmidt, G.A., Mann, M.E., Rind, D., Waple, A., 2001. Solar forcing of regional climate change during the Maunder Minimum. Science 294, 2149–2152.

Smith, L.C., MacDonald, G.M., Velichko, A.A., Beilman, D.W., Borisova, O.K., Frey, K.E., Kremenetski, K.V., Sheng, Y., 2004. Siberian peatlands a net carbon sink and global methane source since the early Holocene. Science 303, 353–356.

Stager, J.C., Mayewski, P.A., 1997. Abrupt early to mid-Holocene climatic transition registered at the Equator and the Poles. Science 276, 1834–1836.

Starkel, L., 1998. Geomorphic response to climatic and environmental changes along a Central Asian transect during the Holocene. Geomorphology 23, 293–305.

Steinke, S., Kienast, M., Pflaumann, U., Weinelt, M., Stattegger, K., 2001. A high-resolution sea-surface temperature record from the tropical South China Sea (16,500–3000 yr BP). Quat. Res. 55, 352–362.

Stott, L., Poulsen, C., Lund, S., Thunell, R., 2002. Super ENSO and global climate oscillations at millennial time scales. Science 297, 222–226.

Stuiver, M., Reimer, P.J., Bard, E., Beck, J.W., Burr, G.S., Hughen, K.A., Kromer, B., McCormac, F.G., v.d.Plicht, J., Spurk, M., 1998. INTCAL98 radiocarbon age calibration, 24,000–0 cal BP. Radiocarbon 40, 1041–1083.

Sun, X.J., Du, N.Q., Weng, C.Y., Lin, R.F., Wei, K.Q., 1994. Paleovegetation and paleoenvironment of Lake Manas, Xinjiang, NW China during the last 14,000 years. Quat. Sci. 3, 239–248 (in Chinese).

Thompson, L.G., Yao, T., Davis, M.E., Henderson, K.A., Mosley-Thompson, E., Lin, P.-N., Beer, J., Synal, H.-A., Cole-Dai, J., Bolzan, J.F., 1997. Tropical climate instability: the last glacial cycle from a Qinghai–Tibetan ice core. Science 276, 1821–1825.

Wagner, F., Bohncke, S.J.P., Dilcher, D.L., Kürschner, W.M., van Geel, B., Visscher, H., 1999. Century-scale shifts in early Holocene atmospheric CO_2 concentration. Science 284, 1971–1973.

Wang, L., Sarnthein, M., Erlenkeuser, H., Grimalt, J., Grootes, P., Heilig, S., Ivanova, E., Kienast, M., Pelejer, C., Pflaumann, U., 1999. East Asian Monsoon climate during the late Pleistocene: high resolution sediment records from the South China Sea. Mar. Geol. 156, 245–284.

Wang, Y.J., Cheng, H., Edwards, R.L., An, Z.S., Wu, J.Y., Shen, C.-C., Dorale, J.A., 2001. A high-resolution absolute-dated Late Pleistocene monsoon record from Hulu cave, China. Science 294, 2345–2348.

Wang, N.L., Yao, T.D., Thompson, L.G., Henderson, K.A., Davis, M.E., 2002. Evidence for cold events in the early Holocene from the Guliya ice core, Tibetan Plateau, China. Chin. Sci. Bull. 47 (17), 1422–1427.

Wei, K., Gasse, F., 1999. Oxygen isotopes in lacustrine carbonates of West China revisited: implications for post glacial changes in summer monsoon circulation. Quat. Sci. Rev. 18, 1315–1334.

Wu, W.X., Liu, D.S., 2004. Possible role of the "Holocene Event 3" on the collapse of Neolithic Cultures around the Central Plain of China. Quat. Int. 117, 153–166.

Wu, J.L., Shen, J., Wang, S.M., Jin, Z.D., Yang, X.D., 2003. Early Holocene climate and environmental characteristics recorded in Aibi lake sediment, Xinjiang. Sci. China, Ser. D 33 (6), 569–575 (in Chinese).

Wünnemann, B., Chen, F.H., Riedel, F., Zhang, C.J., Mischke, S., Chen, G.J., Demske, D., Jin, M., 2003. Holocene lake deposits of Bosten Lake, southern Xinjiang, China. Chin. Sci. Bull. 48 (14), 1429–1432.

Xiao, J.L., Nakamura, T., Lu, H.Y., Zhang, G.Y., 2002. Holocene climate changes over the desert-loess transition of north-central China. Earth Planet. Sci. Lett. 197, 11–18.

Yang, X.P., 2000. Landscape evolution and changes in precipitation in the Badain Jaran Desert since 30000 yr BP. Chin. Sci. Bull. 45 (4), 428–433 (in Chinese).

Yang, X.P., Williams, M.A.J., 2003. The ion chemistry of lakes and late Holocene desiccation in the Badain Jaran Desert, Inner Mongolia, China. Catena 51 (1), 45–60.

Yang, B., Bräuning, A., Shi, Y.F., 2003. Late Holocene temperature fluctuations on the Tibetan Plateau. Quat. Sci. Rev. 22, 2335–2344.

Yang, T.B., Yu, Y.T., Li, J.J., An, C.R., Liu, J.F., Zhang, J.Y., 2004a. Paleomagnetic excursions recorded in the Yanchi playa in middle Hexi Corridor, NW China since the last Interglacial. J. Mount. Sci. 1 (2), 128–142.

Yang, X.P., Rost, K.T., Lehmkuhl, F., Zhu, Z.D., Dodson, J., 2004b. The evolution of dry lands in northern China and in the Republic of Mongolia since the Last Glacial Maximum. Quat. Int. 118/119, 69–85.

Zhang, H.C., Ma, Y.Z., Wünnemann, B., Pachur, H.-J., 2000. A Holocene climatic record from arid northwestern China. Palaeogeogr. Palaeoclimatol. Palaeoecol. 162, 389–401.

Zhou, W.J., Lu, X.F., Wu, Z.K., Deng, L., Jull, A.J.T., Donahue, D., Beck, W., 2002. Peat record reflecting Holocene climatic change in the Zoigê Plateau and AMS radiocarbon dating. Chin. Sci. Bull. 47 (1), 66–70.